European Journal of Medicinal Chemistry 44 (2009) 2044–2051

Contents lists available at ScienceDirect

European Journal of Medicinal Chemistry

journal homepage: http://www.elsevier.com/locate/ejmech

Original article

Synthesis and DNA-binding studies of two ruthenium(II) complexes of an intercalating ligand

D. Lawrence Arockiasamy, S. Radhika, R. Parthasarathi, Balachandran Unni Nair*

Chemical Laboratory, Central Leather Research Institute, Council of Scientific and Industrial Research, Chennai 600 020, India

ARTICLE INFO

Article history:
Received 11 January 2008
Received in revised form
5 June 2008
Accepted 9 October 2008
Available online 1 November 2008

Keywords:
Ruthenium(II) complexes
DNA
Polypyridyl
Photocleavage
Ethidium bromide

ABSTRACT

Two new ruthenium(II) complexes $[Ru(bpy)_2(HBT)]^{2+}$ (**1**) and $[Ru(phen)_2(HBT)]^{2+}$ (**2**) (bpy = 2,2′-bipyridine; phen = 1,10-phenanthroline; HBT = 11*H*, 13*H*-4, 5,9,10,12,14-hexaaza-benzo [*b*] triphenylene) have been synthesized and characterized by elemental analysis, mass spectra, ^{1}H NMR and cyclic voltammetry. The DNA binding property of the two complexes has been investigated employing absorption spectroscopy, fluorescence spectroscopy and viscosity measurements. Both complexes **1** and **2** have been found to prefer intercalative binding to DNA. The DNA binding constants for the two complexes have been measured to be $5.71 \pm 0.20 \times 10^7$ and $4.65 \pm 0.20 \times 10^7$ M^{-1} through ethidium bromide displacement method. Molecular modeling studies too indicate that both complexes **1** and **2** prefer intercalative binding to DNA and both these complexes exhibit similar DNA binding energies. Both complexes **1** and **2** bring about photocleavage of plasmid DNA when irradiated at 440 nm.

© 2008 Elsevier Masson SAS. All rights reserved.

1. Introduction

Studies on the interaction of transition metal complexes with DNA continue to attract the attention of researchers due to their importance in design and development of synthetic restriction enzymes, chemotherapeutic drugs and DNA foot printing agents [1–8]. In this respect ruthenium(II) complexes have attracted a great deal of attention due to their unique spectroscopic and electrochemical properties [9–18]. Ruthenium polypyridyl complexes have received special attention due to their strong metal to ligand charge transfer (MLCT) absorption, their unique emission characteristics, the perturbance of which could be exploited to study their DNA binding properties [19–27]. Despite a considerable amount of literature on metal complex–DNA interaction, the knowledge of the nature of binding of these complexes to DNA and their binding geometries has remained a subject of intense debate. The binding mode of $[Ru(phen)_3]^{3+}$ remains as an issue of rigorous debate [28,29]. On the other hand there is a consensus about intercalative binding of complexes such as $[Ru(bpy)_2(dppz)]^{2+}$ and $[Ru(phen)_2(dppz)]^{2+}$(dppz = dipyrido[3,2-*a*:2′,3′-*c*]-phenazine) to DNA. In these two complexes dppz ligand has been shown to intercalate between the base pairs of double helical DNA [30–35]. It has also been realized that the molecule can intercalate either through the major groove or through the minor groove due to small modifications in the intercalating ligand. The complex $[Ru(phen)_2(dppz)]^{2+}$ has been shown to intercalate into the major groove of double helix DNA [36,37] while $[Ru(phen)_2(dpq)]^{2+}$ (dpq = dipyrido[3,2-*d*:2′,3′-*f*]quinoxaline) intercalates preferentially into the minor groove of DNA [38,39].

Ever since the report of the DNA base mismatch recognition agent, $[Ru(bpy)_2(chrysi)]^{3+}$ (chrysi = 5,6-chrysenequinone diimine), there has been renewed interest in the synthesis of mixed ligand complexes of ruthenium. The complex $[Ru(bpy)_2(chrysi)]^{3+}$ has been found to bind at the mismatch sites in DNA specifically and upon photoactivation cleaves the DNA backbone neighbouring the site [40]. The source of preferential binding has been reported to be the sterically bulky chrysi intercalating ligand, which is too wide to intercalate readily in to B-form DNA, but binds the destabilized regions associated with base mismatches [41]. In our laboratory, we have initiated a systematic study to understand the role of ancillary ligands in the DNA binding mode of mixed ligand complexes of ruthenium(II) and to develop base mismatch recognition agent [42]. In this communication, we describe the synthesis and DNA binding properties of two new ruthenium(II) mixed ligand complexes.

Abbreviations: Bpy, 2,2-bipyridine; Phen, 1,10-phenanthroline; HBT, 11*H*, 13*H*-4, 5,9,10,12,14-Hexaaza-benzo [*b*] triphenylene; dppz, dipyrido[3,2-*a*:2′,3′-*c*]-phenazine; dpq, dipyrido[3,2-*d*:2′,3′-*f*]quinoxaline; chrysi, 5,6-chrysenequinone diimine; tris, tris(hydroxymethyl) aminomethane; CT, calf thymus; DMSO, dimethyl sulfoxide; DIP, 4,7-diphenyl-1,10-phenanthroline; DMHBT, 11,13-dimethyl-4, 5,9,10,12,14-hexaaza-benzo [*b*] triphenylene-10,12-dione.

* Corresponding author. Tel.: +91 44 2441 1630; fax: +91 44 2491 1589.
E-mail address: bunair@clri.info (B.U. Nair).

0223-5234/$ – see front matter © 2008 Elsevier Masson SAS. All rights reserved.
doi:10.1016/j.ejmech.2008.10.013

2. Results and discussion

2.1. Synthesis and characterization

Complexes **1** and **2** could be prepared in 60% yield by prolonged heating of the ligand HBT with *cis*-[Ru(bpy)$_2$Cl$_2$] and *cis*-[Ru(phen)$_2$Cl$_2$], respectively, as shown in Scheme 1. Both the complexes were purified by column chromatography using alumina as the support phase and methanol as the mobile phase. The authenticities of the complexes were ascertained through ^{1}H NMR spectroscopy and electrospray mass spectroscopy. Complexes **1** and **2** show molecular ion peaks at *m*/*z* of 349 and 373, respectively, for the dipositive complex cations. The electronic spectra of complexes **1** and **2** consist of a number of well-defined bands in the range 220–500 nm (Table 1). The spectra were assigned by comparison to that of [Ru(bipy$_2$)]$^{2+}$ and [Ru(phen$_2$)]$^{2+}$. In the case of complex **1** the band observed at 286 nm can be assigned to ligand centered excited states (π_{bpy}–π^*_{bpy} transition) and the band at 364 nm to the π–π^* transition of the HBT ligand. The metal to ligand charge transfer (MLCT) d–π^* transition appear from a complex manifold of energy levels spread over from 370 to 500 nm. The 419 nm band is associated with excitation to 2,2′-bipyridine [43], while the 458 nm band is associated with metal to ligand charge transfer to the BHT ligand. Similarly in the case of complex **2**, the band at 265 nm can be assigned to phenanthroline centered π–π^* transitions. The BHT ligand centered π–π^* transition and the d–π^* transition from the metal to phenanthroline appear together as a broad shoulder between 360 and 390 nm in this case. The d–π^* transition from metal to BHT ligand appears at 453 nm.

Both complexes **1** and **2** have been found to show fluorescence emission from their ^{3}MLCT state upon excitation at 400 nm. The emission bands are centered at 600 and 602 nm in the case of complexes **1** and **2,** respectively. It is interesting to note that analogous complexes [Ru(bpy)$_2$(DMHBT)]$^{2+}$ (where DMHBT is 11,13-dimethyl-13*H*-4,5,9,11,14-hexaaza-benzo[*b*]triphenylene-10,12-dione) show two emission bands (520 and 607 nm) when excited at 440 nm [42]. The complex Ru(DIP)$^{2+}$ (where DIP is 4,7-diphenyl-1,10-phenanthroline) too shows two emission from its ^{3}MLCT state [44]. Both complexes **1** and **2** show quasi reversible electrochemical wave in acetonitrile medium attributable to Ru(II)/Ru(III) couple as shown in Fig. 1. Complex **1** shows oxidation of from Ru(II) to Ru(III) at an anodic peak potential of 1.03 V vs SCE and the corresponding reduction wave at 0.94 V vs SCE with an $E_{1/2}$ of 0.98 V. Complex **2** on the other hand shows anodic wave at 1.12 V vs SCE and the corresponding cathodic wave at 1.06 V vs SCE with an $E_{1/2}$ of 1.09 V. The observed difference of 11 mV in the $E_{1/2}$ of the two complexes can be attributed to the nature of the ancillary ligand. Besides the metal centered redox waves both these complexes show multiple redox waves associated with ligands from 0.04 V to −1.6 V.

2.2. DNA binding studies

2.2.1. Fluorescence intercalated displacement binding assay

The DNA binding constants were determined employing fluorescence intercalator displacement method. Ethidium bromide, a classical intercalator with DNA binding constant in the order of 10^7 [45], displays a dramatic enhancement of its emission intensity when intercalated into DNA due to strong stacking interaction between the adjacent base pairs. This enhanced fluorescence of the DNA–EB complex can be quenched by the addition of a second DNA binder which is either an intercalator [46] or a groove binder [47] and such a decrease in the emission intensity of the pre-bound EB is the basis of the fluorescence intercalator displacement assay. Fig. 2 depicts the variation of emission intensity of the pre-bound EB by the addition of complexes **1** and **2**. As expected, the emission intensity of the pre-bound EB was quenched by the addition of the complex. This could be due to the displacement of the EB molecule from the intercalating site by the ruthenium complex. The binding constant has been estimated to be $5.71 \pm 0.20 \times 10^7$ and $4.65 \pm 0.20 - 10^7$ M^{-1} for complexes **1** and **2**, respectively. The fact that both complexes **1** and **2** show almost similar DNA binding constant indicates that HBT is the intercalating ligand.

2.2.2. Luminescence studies

Emission intensity of complexes **1** and **2** from their MLCT excited states upon excitation at 440 nm, is found to depend on DNA concentration. Fig. 3 shows the emission spectrum of complexes **1** and **2** as a function of DNA concentration. It is interesting to note that while emission intensity of complex **1** shows almost 250% increase in the presence of 80 μM DNA, the emission intensity of complex **2** shows only around 45% increase in the presence of 80 μM DNA. This clearly indicates that complex **1** is in a more

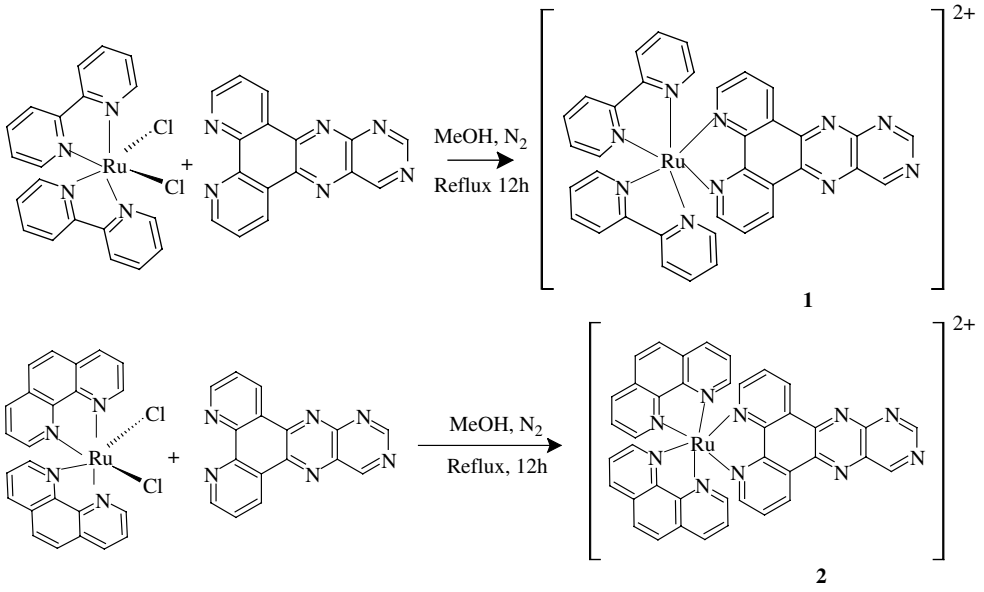

Scheme 1.

Table 1
Spectral parameters of the Ru(II) complexes

Complexes	UV–visible spectrum, λ, nm (log ε)
$[Ru(bpy)_2(HBT)]Cl_2$	244(4.44), 286(4.72), 364(3.95), 419(4.04), 458(4.07)
$[Ru(phen)_2(HBT)]Cl_2$	223(5.00), 265(5.01), 389(4.18), 453(4.26)

hydrophobic environment in the presence of DNA when compared to complex **2**. It is possible that the ancillary ligand 1,10-phenanthroline in complex **2** is more accessible to the bulk solvent because of its slightly larger size compared to the ancillary ligand 2,2′-bipyridine of complex **1**. Similar trend has also been reported for the emission spectrum of complexes $[Ru(bpy)_2(DMHBT)]Cl_2$ and $[Ru(phen)_2(DMHBT)]Cl_2$ in the presence of DNA [42].

2.2.3. Viscosity measurements

Further clarification of the interactions between the ruthenium(II) complexes **1** and **2** and DNA was carried out by viscosity measurements. Optical and photophysical probes provide necessary, but not sufficient, clues to support a binding model. Hydrodynamic measurements that are sensitive to length change (i.e. viscosity and sedimentation) are regarded as the least ambiguous and the most critical tests of a binding model in solution in the absence of crystallographic data. A classical intercalation model demands that the DNA helix must lengthen as base pairs are separated to accommodate the binding ligand, leading to the increase of DNA viscosity. In contrast, a partial and/or non-classical intercalation of ligand bend (or kink) the DNA helix, reduce its length and, concomitantly, its viscosity. Viscosity of CT DNA (200 μM) has been measured in the presence of varying amount of complexes **1** and **2** (20–140 μM). Effect of complexes **1** and **2**, on the viscosity of rod like DNA is depicted in Fig. 4. On increasing the concentration of complexes **1** and **2**, the relative viscosity of DNA increases steadily, which is similar to the behavior of classical intercalator like ethidium bromide and DPPZ. The results suggest that complexes **1** and **2** intercalate between the base pairs of CT DNA.

2.2.4. Molecular modeling

Molecular modeling was carried out to confirm the geometry of the metal complex and its mode of binding to DNA. Minimum energy structures obtained from molecular mechanics calculations are depicted in Fig. 5. The binding energies computed for intercalation through both the minor and major grooves interactions of ruthenium complexes with DNA in the B-conformation are given in Table 2. Optimized structures of Dickerson sequence with both the ruthenium complexes interacted through the intercalation modes are presented in Fig. 6. The binding energy values presented in Table 2 suggest that binding of the complex **1** through the minor groove intercalation of DNA is more favorable by ~6 kcal/mol. For complex **2**, both the intercalated modes through the minor and major grooves are nearly equally favorable. The other noteworthy feature is that there is not much of variation in binding energy for the both metal complex with the Dickerson sequence expect that the binding energy of complex **1** with DNA in major grove intercalation is less than that of respective minor groove intercalation. It is clearly evident from the binding mode shown in Fig. 6 that electrostatic and van der Waals interactions are the dominant interactions, hydrogen bonding interactions having only a minor role and hence, relevant changes in the binding energies of the metal complexes. It is very clear from the binding models in Fig. 6 that when complex **1** intercalates through the minor groove there is a better contact of the pi-cloud of the aromatic ligand with the backbone of DNA than when the same complex intercalates through the major groove and as a result the binding energy of such an interaction is higher than that of its interaction through the major groove. These computations clearly bring out that complex **1** essentially prefers intercalating through the minor groove with a binding energy of −46.25 kcal/mol. The DNA binding energy of complex **2**, irrespective of its intercalation through minor or major groove too is around −46 kcal/mol. These results are in keeping with the binding studies, which also show that the DNA binding constant of both the complexes are nearly the same.

2.2.5. DNA photocleavage

A number of metal polypyridyl complexes have been shown to exhibit DNA photocleaving ability [14,48]. The cleavage of plasmid DNA can be easily monitored by agarose gel electrophoresis. When circular supercoiled plasmid (Form I) DNA is subjected to electrophoresis, relatively fast migration will be observed. If DNA nicking occurs at one strand the supercoiled DNA will relax to generate slow moving open circular form (Form II). If both strands are cleaved, a linear form (Form III) that migrates between Form I and Form II will be generated. Both complexes **1** and **2** have been found to bring about photocleavage of supercoiled plasmid pBR 322 when

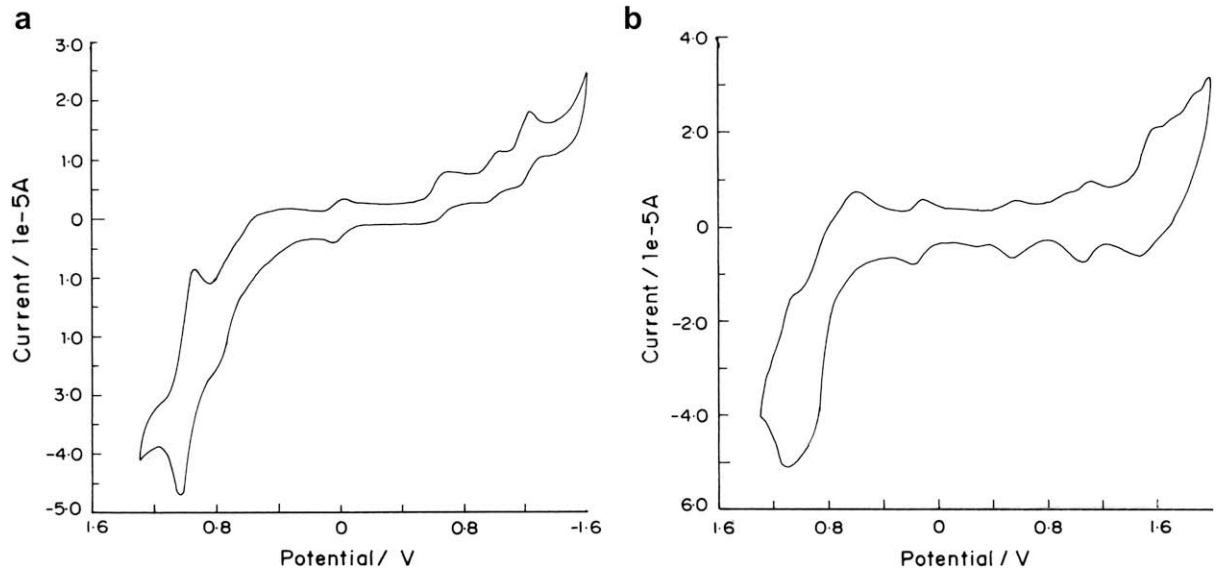

Fig. 1. Cyclic Voltammogram of 2 mM solution of complex **1** (a) and complex **2** (b) in acetonitrile in the presence of 0.1 M tetrabutylammonium perchlorate. Scan rate 0.1 V s^{-1}.

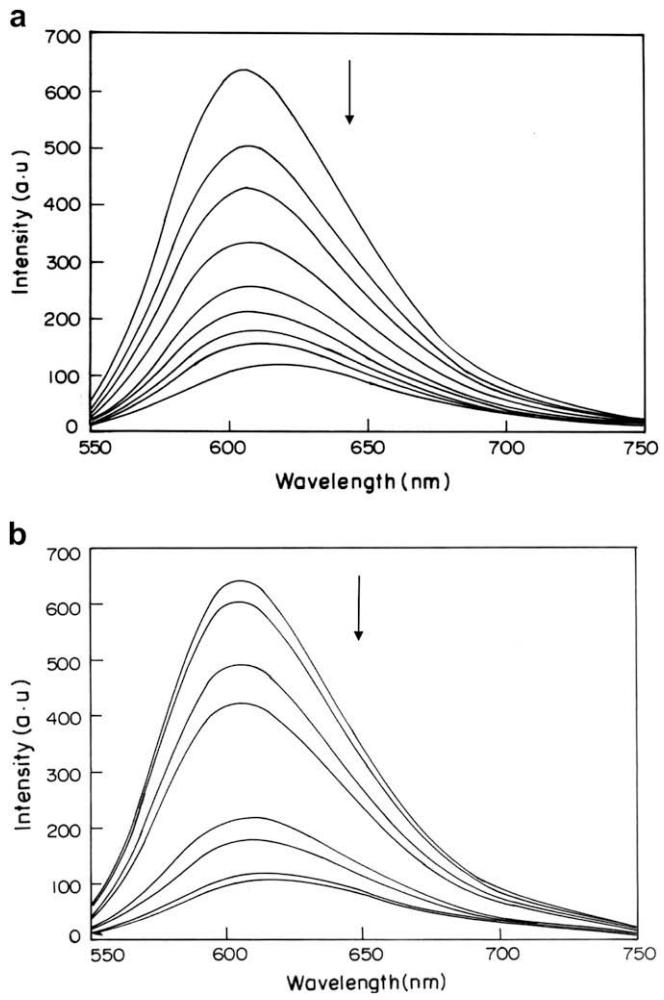

Fig. 2. (a) Emission spectrum of EB(10 μM)–DNA(10 μM) in the presence of increasing amounts (0.5–4 μM) of Complex **1.** Arrow shows the emission intensity change upon increasing the complex concentration (b). Emission spectrum of EB(10 μM)–DNA(10 μM) in the presence of increasing amounts (0.5–4 μM) of Complex **2.** Arrow shows the emission intensity change upon increasing the complex concentration.

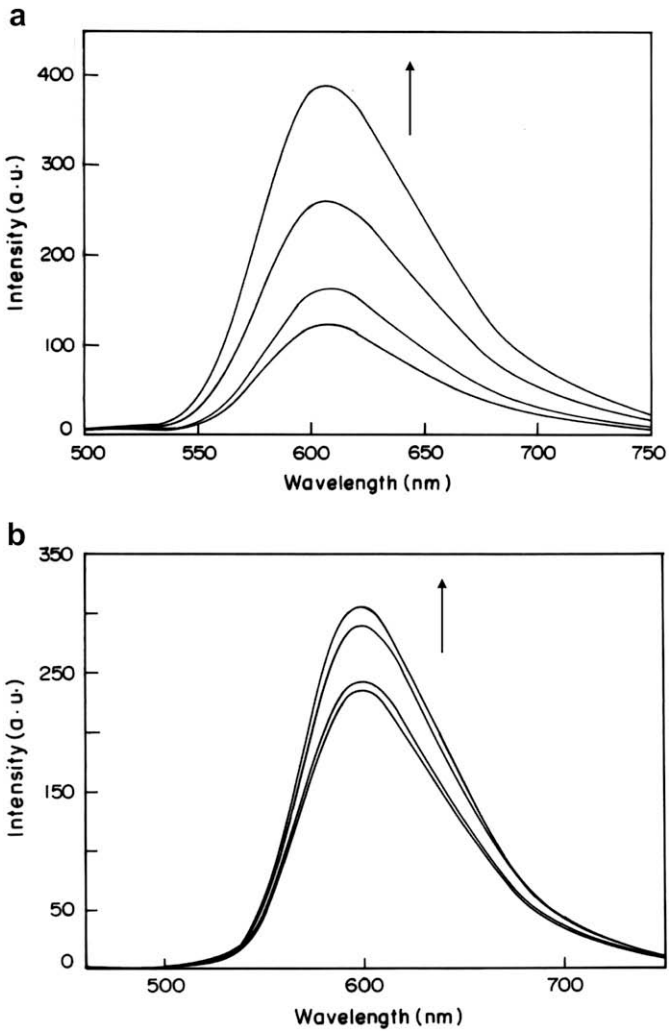

Fig. 3. (a) Emission spectrum of complex **1**(20 μM) in the absence (1) and the presence of 20 (2), 40 (3), 80 (4) μM CT DNA (b). Emission spectrum of complex **2** (20 μM) in the absence (1) and the presence of 20 (2), 40 (3), 80 (4) μM CT DNA.

excited at 440 nm. Fig. 7(a) shows the gel electrophoresis separation of pBR 322 DNA after incubation with complex **1** and irradiation at 440 nm. Control experiment suggests that incubation of complex **1** with plasmid DNA in the dark does not lead to any DNA cleavage (lane 1). Irradiation of DNA alone for 1.5 h also did not lead to any DNA cleavage (lane 2). On the other hand when DNA (200 n gm) was incubated with 3 μL of 1 mM complex **1** prior to illumination at 440 nm, substantial amount of Form II DNA could be seen (lane 3). In order to identify the nature of reactive species that are responsible for the photocleaving activity of the complex, photoexcitation of complex and DNA was also carried out in the presence of singlet oxygen scavenger sodium azide as well as hydroxyl ion scavenger DMSO. Presence of sodium azide did not inhibit the photocleavage of DNA as evident from lane 4 of Fig. 7(a). This is in contrast with what has been observed in the case of $Ru(Phen)_3^{2+}$, where the DNA photocleaving activity of the complex has been attributed to singlet oxygen [49]. The DNA photocleaving ability of complex **1** on the other hand is significantly reduced in the presence of a hydroxyl ion scavenger like DMSO (lane 5). Hence it is clear that hydroxyl radical plays a significant role in the observed DNA photocleaving activity of complex **1**. Similar results have been obtained with complex **2** as can be seen from Fig. 7(b). Both these complexes have been found to be equally efficient photocleavers of DNA.

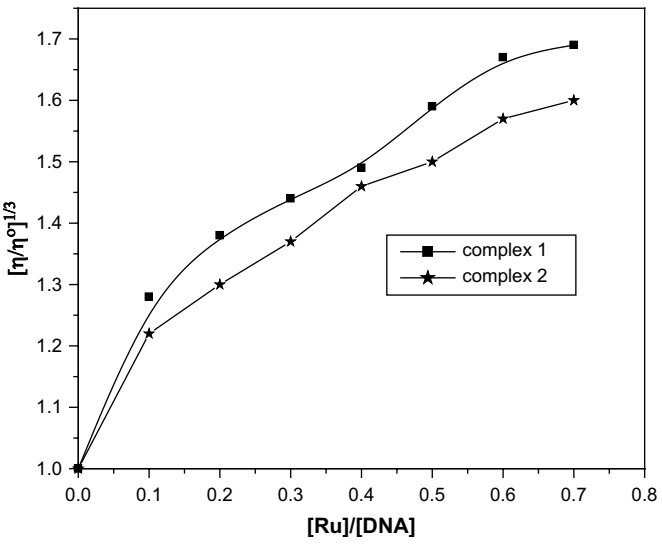

Fig. 4. Effect of increasing amounts (0–40 μM) of complexes **1** and **2** on the relative viscosity of CT DNA (100 μM).

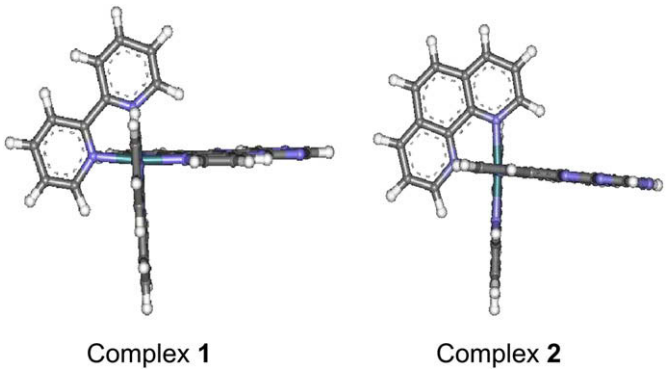

Fig. 5. Energy minimized geometries of Ru(II) complexes.

3. Materials and methods

3.1. Materials

Ruthenium trichloride and calf thymus DNA (CT DNA) were purchased from SRL Chemicals, Mumbai. 1,10-Phenanthroline and 2,2′-bipyridine were purchased from Ranbaxy Chemicals. 4,5-Diaminopyrimidine was purchased from Aldrich Chemicals. LiCl was purchased from SD Fine Chemicals. All other chemicals used were of analytical reagent grade and were used without any further purification.

3.2. Physical measurements

Elemental analysis (C, H, N) was carried out with a Heraeus-CHN-Rapid analyzer at Regional Sophisticated Instrumentation Centre, IIT, Chennai. ^{1}H NMR spectra were recorded on a JEOL ECA-500 spectrometer with CD_3OD as solvent and $SiMe_4$ as an internal standard. Thermo electron LCQAD-60000 electrospray ionization (ESI) mass spectrometer was employed for the investigation of charged metal complex species in acetonitrile solvent. UV–visible spectra were recorded on a Perkin–Elmer Lamda 35 spectrophotometer. Fluorescence measurements were carried out using Cary Eclipse spectrofluorimeter. Ostwald's viscometer was employed for viscosity measurements. Cyclic voltammetry (CV) measurements were carried out using a CH Instruments electrochemical analyzer. The CV experiments were performed in a one-compartment cell equipped with a glassy carbon working electrode and platinum wire as the auxiliary electrode. A saturated calomel electrode (SCE) was used as the reference electrode. Tetrabutylammonium perchlorate (0.1 M) was used as supporting electrolyte.

3.3. DNA binding and cleaving studies

All the experiments involving the interaction of the complexes with DNA were carried out in tris buffer (10 mM, pH 7.5). A stock solution of DNA was prepared by stirring a sample dissolved in 10 mM tris buffer at 4 °C. The filtered DNA solution in the buffer gave a UV absorbance ratio (A_{260}/A_{280}) of ~1.9, indicating that the DNA was sufficiently free from protein [50]. The DNA concentration was determined by measuring the absorption of the DNA solution at 260 nm and employing molar absorption coefficient value of 6600 M^{-1} cm^{-1}. Absorption titration experiments were performed by maintaining the metal complex concentration constant (10 μM) and varying the concentration of nucleic acid from 20 to 200 μM. While measuring the absorption spectra, equal amount of DNA was added to both complex solution and reference solution to eliminate the absorbance of DNA itself. Steady state fluorescence spectroscopic experiments on the interaction of the complexes with CT DNA–ethydium bromide (EB) complex were carried out at 25 °C. The solutions were excited at 335 nm and the fluorescence intensity was measured at 600 nm. The complex of CT DNA (10 μM) and EB (10 μM) in tris buffer (10 mM, pH 7.5) was placed in a thermostated quartz fluorescence cuvette and titrated with aliquots of the ruthenium complexes (to get complex concentration from 0.5 to 4 μM) with continuous stirring. The total volume of the solution was 2 mL. After each titration, the solution was mixed thoroughly and allowed to equilibrate thermally for 5 min prior to fluorescence measurements. The apparent binding constant (K_{app}) has been calculated from the equation: $K_{EB}[EB] = K_{app}$ [Complex], where K_{EB} is 1.0×10^7 M^{-1}. [Complex] was the concentration of the ruthenium complex at which 50% reduction of the emission intensity of pre-bound EB was observed. Fluorescence spectra of the two ruthenium complexes (20 μM) were measured in the presence of 20, 40 and 80 μM DNA solution. Viscometric experiments were carried out using a viscometer of 3 mL capacity, thermostated in water bath maintained at 25 ± 1 °C. The flow rates of the buffer, DNA (200 μM) and DNA in the presence of ruthenium complexes at various concentrations (20–140 μM) were measured with a manually operated timer at least three times to agree within 0.2 s. The relative specific viscosity was calculated according to the relation $\eta = (t - t_0)/t_0$, where 't_0' is the flow time for the buffer and 't' is the observed flow time for DNA in the presence and absence of the ruthenium complex. A plot of $(\eta/\eta^0)^{1/3}$ vs $1/R$ (R = [DNA]/[Complex]) was constructed from viscosity measurements [51].

Gel electrophoresis of plasmid DNA (pBR 322 DNA) was carried out with 25 μL reaction mixture containing 4 μL of 100 μg/mL plasmid DNA, 5 μL of 0.1 mM complexes **1** or **2** and remaining buffer. A 5 μL aliquot of NaN_3 solution was added to one of the samples. The metal complex–DNA solution was preincubated for 1 h in the dark and the samples were kept in the spectrofluorimeter sample chamber. The samples were then irradiated at 440 nm. The samples were subsequently analyzed by 0.8% agarose gel electrophoresis (Tris–boric acid–EDTA buffer, pH 8.0) at 50 V for 4 h. The gel was stained with 0.5 μg/mL ethidium bromide. The stained gel was illuminated under a UV lamp and photographed.

Table 2
Calculated binding energies of Ru(II) complexes with polynucleotides through molecular modeling

Complex	Intercalation through	Biding energy (kcal/mol)
1	Major groove	−40.45
	Minor groove	−46.25
2	Major groove	−46.41
	Minor groove	−46.77

3.4. Molecular modeling

Molecular modeling was performed on a Silicon Graphics O2 workstation using the Biosym Modeling package from Molecular Simulation Inc. (SanDiego, CA). The B-DNA system chosen for the study was the dodecamer duplex of sequence $d(CGCGAATTCGCG)_2$ and constructed using the Biopolymer program of the Insight II package. Both complexes **1** and **2** were constructed with the builder module of Insight II, and energy optimization was performed using an extensible systematic force field (ESFF) with the Discover3 program. The metal complexes and each metal/B-DNA complex were subjected to minimization using ESFF with a non-bonded cutoff of 10 Å and a sigmoidal distant-dependent dielectric function ($\varepsilon = 4r_{ij}$), which had been demonstrated to be an appropriate implicit treatment for the dielectric function in computing the electrostatic potential of nucleic acid. In the energy minimization, the geometry of the whole complex was then refined until convergence (criterion of root mean square (rms) energy gradient of 0.01 kcal/mol per Å) was reached throughout. The interaction

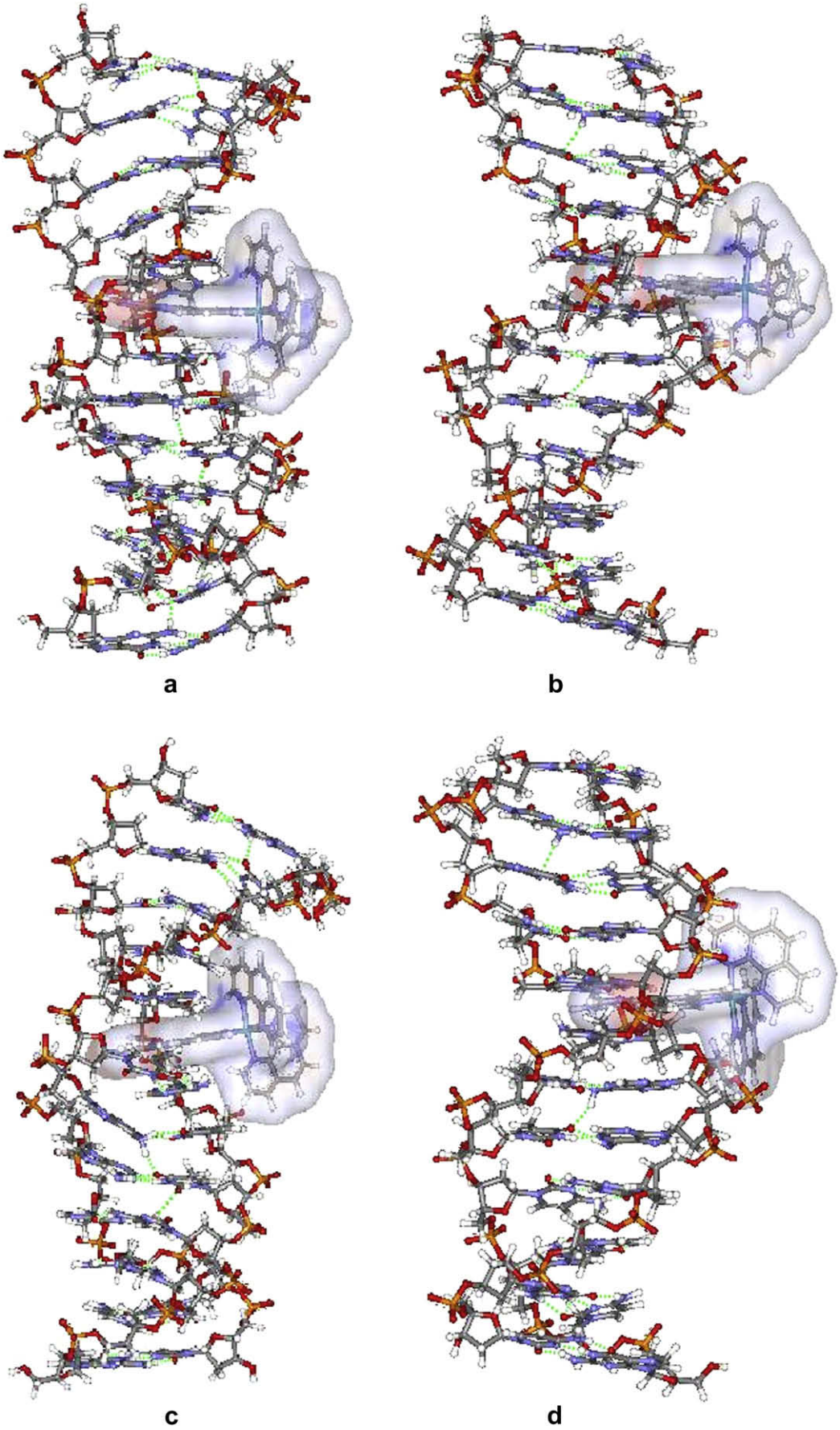

Fig. 6. Intercalation of complex **1** through (a) major groove and (b) minor groove. Intercalation of complex **2** through (c) major groove and (d) minor groove.

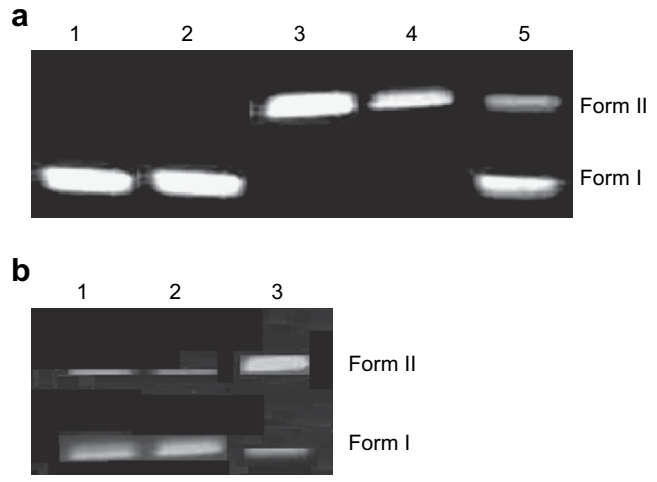

Fig. 7. (a)Gel electrophoresis separation of pBR 322 DNA after incubation with complex **1** and irradiation at 440 nm. DNA + complex **1** dark (lane 1), DNA irradiated for 1.5 h (lane 2), DNA + complex **1** irradiated for 1.5 h (lane 3), DNA + complex **1** + sodium azide irradiated for 1.5 h (lane 4), DNA + complex **1** + DMSO irradiated for 1.5 h (lane 5) (b). Gel electrophoresis separation of pBR 322 DNA after incubation with complex **2** and irradiation at 440 nm. DNA + complex **2** dark (lane 1), DNA irradiated for 1.5 h (lane 2), DNA + complex **1** irradiated for 1.5 h (lane 3).

energy of the metal–DNA complex was estimated from the difference between their total energies and the sum of lowest energies found for the optimized structures of the free DNA and the metal complex. The negative of the interaction energy gives the binding energy: IE = TE − (sum individual energies of DNA and Metal), BE = −IE where IE is the interaction energy, TE the total energy of the Ru–DNA complex, and BE the binding energy.

To obtain further support for the DNA binding mode, the binding energies of the metal complex were calculated with the Dickerson sequence, $d(GCGCATATGCGC)_2$. Since energy minimization studies show that the intercalative binding mode seems to be more stable for both the metal complexes than the major/minor groove binding modes, it was manually docked at different intercalative sites of the B-form DNA. Several possible starting geometries for intermolecular complexes were selected by a structure-based docking strategy and by considering all possible steric factors. The complex was positioned in all possible modes of the binding viz. intercalation through both the minor and major grooves. It is evident from previous reports on the interaction of various metal complexes with DNA that extensible systematic force field (ESFF) provides reliable estimates of the binding energy, and a possible comparison with the experimental results can be rationalized.

3.5. Synthesis of the complexes

3.5.1. Synthesis of *11*H, *13*H-*4, 5,9,10,12,14-hexaaza-benzo [*b*] triphenylene (HBT)*

1,10-Phenathroline 5,6-dione was prepared according to the reported procedure. 1,10-Phenathroline 5,6-dione (0.5 g, 2.38 mmol) was dissolved in 50 mL of hot ethanol. To this, ethanolic solution of 0.6 g (2.38 mmol) of 4,5-diaminopyrimidine was added. This mixture was refluxed for 12 h at 80 °C and the precipitate formed was filtered and washed with diethyl ether. It was recrystallised from hot ethanol–acetonitrile (5:1) mixture. The purity of the product was ascertained through TLC.

3.5.2. Synthesis of $[Ru(L)_2(HBT)]Cl_2$ (L = bby for **1** and phen for **2**)

[*cis*-$(bby)_2$ $RuCl_2]\cdot 2H_2O$ and [*cis*-$(phen)_2$ $RuCl_2]]\cdot 2H_2O$ required for synthesis of **1** and **2** were prepared according to reported procedure [52]. Synthesis of $[Ru(L)_2(HBT)]Cl_2$ (where L = bpy or phen) was as follows. The starting material [*cis*-$(bby)_2$ $RuCl_2]]\cdot 2H_2O$ or [*cis*-$(phen)_2$ $RuCl_2]]\cdot 2H_2O$ (0.152 mmol) and HBT (0.152 mmol) were heated to reflux in 25 mL methanol for 12 h under nitrogen atmosphere. This solution was cooled to room temperature, filtered and the solvent was removed from the filtrate using rotary evaporator. The dark brown solid isolated was washed with acetone and dried. The product could be satisfactorily purified by chromatography on alumina gel by using CH_3CN–CH_3OH solution ((95:5, v/v) as the eluent.

$[Ru(bpy)_2(HBT)]Cl_2$: yield 72%. Anal. Calc. for $C_{36}H_{24}N_{10}Ru$: C, 72.47; H, 4.05; N, 23.48. Found: C, 72.52; H, 4.01; N, 23.3. ^{1}NMR (CD_3OD): 8.83–8.89 (multiplet (m), 4H), 8.21–8.29 (m, 4H), 8.10–8.20 (m, 4H), 7.80–7.87 (m, 4H), 7.54–7.64 (doublet (d), 4H, $J = 6.8$ Hz,), 7.33–7.43, (m, 4H), $m/z = 348.8$.

$[Ru(phen)_2(HBT)]Cl_2$: yield 76%. Anal. Calc. for $C_{40}H_{22}N_{10}$ Ru: C, 74.52; H, 3.75; N, 21.73. Found: C, 74.62; H, 3.71; N, 21.68. ^{1}NMR (CD_3OD): 10.4 (doublet (d), 1H), $J = 4.6$ Hz), 10.2 (d, 2H, $J = 4$ Hz), 9.8 (d, 1H, $J = 5.15$ Hz), 8.8 (triplet(t), 4H, $J = 8.55$ Hz), 8.6 (multiplet (m), 4H), 8.2 (multiplet (m), 4H), 8.1 (multiplet (m), 2H), 7.7 (multiplet (m), 2H), 7.5 (doublet of a doublet (dd), 2H, $J_1 = 5.4$ Hz), 7.3 (dd, 2H, $J_1 = 5.4$ Hz, $J_2 = 8.8$ Hz), $m/z = 372.8$.

References

[1] A. Sigel, H. Sigel (Eds.), vol. 33, Marcel Dekker, New York, (996)177-252.
[2] K.E. Erkkila, D.T. Odom, J.K. Barton, Chem. Rev. 99 (1999) 2777–2796.
[3] L.N. Ji, X.H. Zou, J.G. Liu, Coord. Chem. Rev. 216–217 (2001) 513–536.
[4] V.G. Vaidyanathan, B.U. Nair, Dalton Trans. (2005) 2842–2848.
[5] P.P. Pelligrini, J.R. Aldrich-Wright, Dalton Trans. (2003) 176–183.
[6] P.U. Maheswari, M. Palaniandavar, Inorg. Chim. Acta 357 (2004) 901–912.
[7] X.J. Yang, F. Drepper, B. Wu, W.H. Sun, W. Haehnel, C. Janiak, Dalton Trans. (2005) 256–267.
[8] L.-F. Tan, F. Wang, H. Chao, Y.-F. Zhou, C. Weng, J. Inorg. Biochem. 101 (2007) 700–708.
[9] H. Xu, K.C. Zheng, Y. Chen, Y.Z. Li, L.J. Lin, H. Li, P.X. Zhang, L.N. Ji, Dalton Trans. (2003) 2260–2268.
[10] F.R. Liu, K.Z. Wang, G.Y. Bai, Y.A. Zhang, L.H. Gao, Inorg. Chem. 43 (2004) 1799–1806.
[11] A. Ambroise, B.G. Maiya, Inorg. Chem. 39 (2000) 4264–4272.
[12] Y.-J. Liu, H. Chao, L.-F. Tan, Y.-X. Yuan, W. Wei, L.-N. Ji, J. Inorg. Biochem. 99 (2005) 530–537.
[13] A.C. Benniston, V. Grosshenny, A. Harriman, R. Ziessel, Dalton Trans. (2004) 1227–1232.
[14] L.-F. Tan, H. Chao, H. Li, Y.-J. Liu, B. Sun, W. Wei, L.-N. Ji, J. Inorg. Biochem. 99 (2005) 513–520.
[15] J.A. Smith, J.G. Collins, B.T. Patterson, F.R. Keene, Dalton Trans. (2004) 1277–1283.
[16] J.Z. Wu, L. Yuan, Y. Yu, Inorg. Chim. Acta 359 (2006) 718–720.
[17] P.J. Dandliker, R.E. Holmlin, J.K. Barton, Science 275 (1997) 1465–1468.
[18] X.-J. Yang, C. Janiak, J. Heinze, F. Drepper, P. Mayer, H. Piotrowski, P. Klufers, Inorg. Chim. Acta 318 (2001) 103–116.
[19] J.G. Liu, B.H. Ye, H. Li, L.-N. Ji, R.H. Li, J.Y. Zhou, J. Inorg. Biochem. 73 (1999) 117–122.
[20] H. Chao, J.-G. Liu, L.-N. Ji, X.-Y. Li, J. Biol. Inorg. Chem. 6 (2001) 143–150.
[21] K. Karidi, A. Garoufis, N. Hadjiliadis, J. Reedijk, Dalton Trans. 728–734 (2005).
[22] H. Deng, H. Xu, Y. Yang, H. Li, H. Zou, L.H. Qu, L.-N. Ji, J. Inorg. Biochem. 97 (2003) 207–214.
[23] K. Karidi, J. Reedijk, N. Hadjiliadis, A. Garoufis, J. Inorg. Biochem. 101 (2007) 1483–1491.
[24] T. Biver, C. Cavazza, F. Secco, M. Venturini, J. Inorg. Biochem. 101 (2007) 461–469.
[25] L.-F. Tan, X.-H. Liu, H. Chao, L.-N. Ji, J. Inorg. Biochem. 101 (2007) 56–63.
[26] M.T. Mongelli, J. Heinecke, S. Mayfield, B. Okyere, B.S.J. Winkel, J. Brewer, J. Inorg. Biochem. 100 (2006) 1983–1987.
[27] V.G. Vaidyanathan, B.U. Nair, J. Inorg. Biochem. 91 (2002) 405–412.
[28] S. Satyanarayana, J.C. Dabrowiak, J.B. Chaires, Biochemistry 32 (1993) 2573–2584.
[29] J.E. Coury, J.R. Anderson, L. McFail-Isom, L.D. Williams, L.A. Battenly, J. Am. Chem. Soc. 119 (1997) 3792–3796.
[30] C. Turro, S.H. Bossman, Y. Jenkins, J.K. Barton, W.J. Turro, J. Am. Chem. Soc. 117 (1995) 9026–9032.
[31] E. Tuite, P. Lincoln, B. Norden, J. Am. Chem. Soc. 119 (1997) 239–240.
[32] S.J. Moon, J.M. Kim, J.Y. Choi, S.K. Kim, J.S. Lee, H.G. Jang, J. Inorg. Biochem. 99 (2005) 994–1000.
[33] Q.-X. Zhen, Q.-L. Zhang, J.-G. Liu, B.-H. Ye, L.-N. Ji, L. Wang, J. Inorg. Biochem. 79 (2000) 285–293.
[34] X.-H. Zou, B.-H. Ye, J.-G. Liu, Y. Xiong, L.-N. Ji, Dalton Trans. (1999) 1255–1263.
[35] C.-W. Jang, H. Chao, R.-H. Li, L.-N. Ji, Polyhedron 20 (2001) 2187–2193.
[36] C.M. Dupurer, J.K. Barton, J. Am. Chem. Soc. 116 (1994) 10286–10287.
[37] C.M. Dupurer, J.K. Barton, Inorg. Chem. 36 (1997) 33–43.

[38] I. Greguric, J.R. Aldrich-Wright, J.G. Collins, J. Am. Chem. Soc. 119 (1997) 3621–3622.
[39] J.G. Collins, A.D. Sleeman, J.R. Aldrich-Wright, I. Greguric, T.W. Hambley, Inorg. Chem. 37 (1998) 3133–3141.
[40] B.A. Jackson, J.K. Barton, Biochemistry 39 (2000) 6176–6182.
[41] B.A. Jackson, V.Y. Alckscyev, J.K. Barton, Biochemistry 38 (1999) 4655–4662.
[42] D. Lawrence, V.G. Vaidyanathan, B.U. Nair, J. Inorg. Biochem. 100 (2006) 1244–1251.
[43] A. Juris, S. Barigelletti, S. Campagna, V. Balzani, P. Belser, A. Von Zelewsky, Coord. Chem. Rev. 84 (1988) 85–277.
[44] C.V. Kumar, J.K. Barton, N. Turro, J. Am. Chem. Soc. 107 (1985) 5518–5523.
[45] M. Lee, A.L. Rhodes, M.D. Wyatt, S. Forror, J.A. Hartley, Biochemistry 32 (1993) 4237–4255.
[46] V.G. Vaidyanathan, B.U. Nair, J. Inorg. Biochem. 95 (2003) 334–342.
[47] Y.H. Shim, P.B. Arimondo, A. Laigle, A. Garbesi, S. Lavielle, Org. Biomol. Chem. 2 (2004) 916–921.
[48] A. Hergueta-Bravo, M.E. Jimenez-Hernandez, F. Montero, E. Oliveros, G. Orellana, J. Phys. Chem. B 106 (2002) 4010–4017.
[49] H.Y. Mei, J.K. Barton, Proc. Natl. Acad. Sci. U.S.A. 85 (1988) 1339–1347.
[50] J. Marmur, J. Mol. Biol. 3 (1961) 208–218.
[51] G. Cohen, H. Eisenberg, Biopolymers 8 (1969) 45–55.
[52] B.P. Sullivan, D.J. Salmon, T.J. Meyer, Inorg. Chem. 17 (1978) 3334–3341.